New archaeomagnetic directions from Portugal and evolution of the geomagnetic field in Iberia from Late Bronze Age to Roman Times.

A. Palencia-Ortas, M.L. Osete, S.A. Campuzano, G. McIntosh, J. Larrazabal, J. Sastre, J. Rodriguez-Aranda

PII: S0031-9201(17)30004-3
DOI: http://dx.doi.org/10.1016/j.pepi.2017.07.004
Reference: PEPI 6064

To appear in: *Physics of the Earth and Planetary Interiors*

Received Date: 10 January 2017
Revised Date: 7 July 2017
Accepted Date: 18 July 2017

Please cite this article as: Palencia-Ortas, A., Osete, M.L., Campuzano, S.A., McIntosh, G., Larrazabal, J., Sastre, J., Rodriguez-Aranda, J., New archaeomagnetic directions from Portugal and evolution of the geomagnetic field in Iberia from Late Bronze Age to Roman Times., *Physics of the Earth and Planetary Interiors* (2017), doi: http://dx.doi.org/10.1016/j.pepi.2017.07.004

New archaeomagnetic directions from Portugal and evolution of the geomagnetic field in Iberia from Late Bronze Age to Roman Times.

A. Palencia-Ortas[1,2]; M.L. Osete[1,2]; S. A. Campuzano[1,2]; G. McIntosh[3]; J. Larrazabal[4]; J. Sastre[5]; J. Rodriguez-Aranda[1]

(1) Universidad Complutense de Madrid. Dpto. Física de la Tierra, Astronomía y Astrofísica I. Madrid (Spain).

(2) Instituto de Geociencias, CSIC – UCM. Madrid (Spain).

(3) School of Human and Life Sciences. Canterbury Christ Church University. Canterbury (The United Kingdom).

(4) Lab2PT, Universidade do Minho (Portugal).

(3) ACE Baixo Sabor (Portugal).

Summary:

This study presents new archaeomagnetic results from 33 combustion structures (kilns and hearths) from the archaeological sites of Castelinho, Crestelos, Olival Poço da Barca and Fonte do Milho in NE Portugal. The age of the investigated structures ranges from 1210 BC to 200 AD according to calibrated radiocarbon dating, thermoluminescence dating and archaeological constraints. Stepwise thermal and alternating field demagnetization isolate a single, stable, characteristic remanence component with very well defined directions. Rock magnetic analyses suggest low-Ti titanomagnetite/maghemite as the main magnetic carrier of the remanence. Mean directions are well grouped in most structures. The effect of thermoremanent anisotropy on mean directions has been evaluated and was found to be important. Inclination increases of between 2° and 13° after applying the anisotropy correction at specimen level. This highlights the requirement of evaluating this effect on the directions of small and flattened thin kilns and hearths. The 31 new directional data improve both the temporal and spatial distribution of the Iberian archaeomagnetic dataset from Late Bronze Age to Roman Times. Finally, a new directional palaeosecular variation curve for Iberia for the last twelve centuries BC is proposed. The curve has been computed using the bootstrap method and includes data coming from sites within 900 km of Madrid. The new palaeodirectional secular variation curve for Iberia is consistent with the Western European palaeosecular variation curve and with the prediction of regional European models.

1. Introduction.

Knowledge of the evolution of the ancient geomagnetic field is a crucial topic in geosciences: i) to constrain geodynamo models and therefore to understand the origin of the geomagnetic field, ii) to reconstruct past solar activity based on cosmogenic nuclide production rates (e.g., Muscheler et al., 2007; Usoskin, 2013) which are modulated by the solar and terrestrial magnetic field and iii) to provide chronological constraints of baked archaeological material, volcanic rocks, and Quaternary sediments (e.g., Gallet et al., 2009; Pavón-Carrasco et al., 2011; Roberts et al., 2013).

The variation of the geomagnetic field can be studied directly through observatory and satellite data and extended back to the 17th century AD using historical data. Further in the past, the study of palaeosecular variation of the geomagnetic field (PSV) is based on palaeomagnetic data. The most suitable materials are well-dated archaeological combustion structures (hearths and kilns) and volcanic rocks. Archaeomagnetic data provide the most precise, high-resolution palaeomagnetic data for the last millennia since their thermoremanent magnetization (TRM) is acquired in a short time interval (from hours to days) and they can be well dated using physical as well as archaeological techniques. Data obtained from lava flows, although very useful, can sometimes be problematic, presenting small inclination shallowing or dating problems (for more details, see Lanza et al., 2005; Pavón-Carrasco et al., 2016, and references therein). Palaeomagnetic data coming from sediments may smooth the apparent PSV of the geomagnetic field and could also show inclination shallowing effects (see Tauxe, 1993).

A compilation of archaeomagnetic data allows the construction of a Palaeosecular Variation Curve (PSVC), which then provides knowledge of geomagnetic field variations at regional scales for periods covering the last few millennia. If the PSV curve is well-defined it can be used as a master curve for dating purposes. At present, the secular variation of the geomagnetic field in the Iberian Peninsula is poorly constrained. The published directional Iberian PSVC, centred on Madrid, covering the last 3000 years (Gómez-Paccard et al., 2006b), contains 63 Spanish archaeomagnetic directions (Gómez-Paccard et al., 2006a), 63 data from South France and 9 from North Morocco. The resulting PSVC of Iberia is a mixture of French, Moroccan and Iberian data, but for pre-Roman Times is based exclusively on French data.

In recent years, new studies have been carried out in Iberia, covering the last three millennia (Catanzariti et al., 2008, 2012; Casas et al., 2014; Gómez-Paccard et al., 2008, 2013; Osete et al., 2016; Prevosti et al., 2013; Ruiz-Martínez et al., 2008). However, the extension of the directional curve to the first millennia BC still remains limited by the lack of reliable data. It is also unfortunate that the Iberian PSVC contains no data from Portugal and, despite numerous archaeomagnetic studies carried out during the last decade only one (Catanzariti et al., 2008) is from a Portuguese archaeological site.

This study addresses two of the great issues of the Iberian archaeomagnetic dataset; the scarcity of data for the first millennium BC and the near absence of palaeodirectional data

from Portugal. We present new archaeomagnetic directional data from 33 hearths and kilns from four archaeological sites in northern Portugal, with ages ranging from 1210 BC up to 200 AD. A new Iberian directional PSVC for the period spanning 1200 BC – 200 AD is also proposed.

2. Sampling and laboratory protocols.

The investigated archaeological sites are located in northern Portugal (figure 1a), Castelinho and Olival Poço da Barca (Lat. 41.2° N, Long. 7.0° W), Crestelos (Lat. 41.3° N, Long. 6.9° W) and Fonte do Milho (Lat. 41.1° N, Long. 7.4° W).

The Crestelos site (close to the locality of Meirinhos, figure 1b and 1c) is sub-divided into two excavation areas, an upper area named Povoado de Crestelos (labelled PCR in this study) and a lower area named Quinta de Crestelos (labelled QCR). 12 combustion structures were sampled from PCR and 16 from QCR, including hearths and small kilns (the basal level dimensions of the structures were around 0.5mx0.5m). The preserved part of the combustion structures is the 1-2 cm thick basal level made of a thin layer of flattened smooth clayish sediments (figure 1). Most of them were in a good state of preservation, with the exception of PCR20A and PCR26, which were highly fractured and poorly preserved. On the basis of archaeological information the main occupation of the archaeological site occurred mostly during the Late Iron Age (2nd century BC to 1st century AD).

Olival Poço da Barca and Castelinho are located close to the locality of Felgar. At Olival Poço da Barca (labelled OPB) a large Roman pottery-making kiln was excavated, comprising a rectangular structure with three well-preserved supporting walls (figure 1e). At the Iron Age archaeological site of Castelinho (labeled CAST, figure 1f), three small hearths were sampled. Finally, close to the locality of Canelas, one structure was sampled at the Fonte do Milho archaeological site (labelled FM, figure 1d). The structures sampled at CAST and FM sites are similar to the hearths at PCR and QCR.
Further archaeological and dating details of the sites are given in the AHBS Monography (2014), C2TN Relatorio (2014) and in the Cambridge Publication (in press).

Figure 1: a) Map with the location of the studied archaeological sites, b) Povoado de Crestelos (PCR), c) Quinta de Crestelos (QCR), d) Fonte do Milho (FM), e) Olival Poço da Barca (OPB) and f) Castelinho (CAST).

The surface of most hearths and small kilns was flat and sub-horizontal. North was marked directly on the sample by means of a magnetic compass (see figure 1). Small tilts were considered original rather than post-cooling in most of the structures, but the strike and dip were carefully measured in all cases. In contrast, evidence of post-cooling tilting was observed in the FM and CAST structures, which was probably caused by younger superimposed walls. For these structures the strike and dip was measured.

The plaster of Paris sampling technique was applied for the baked clay blocks sampled from the wall of the OPB kiln and for the baked argillaceous layer from QCR12. This procedure consists of marking magnetic north on a horizontal plaster surface that is adhered to the sample surface. Compass readings have been corrected for the local declination of the studied sites using IGRF. In the laboratory, samples were consolidated by impregnation in sodium silicate (water-glass) and then cut into standard cubic specimens (8 cm^3), or sub-cubic if the thickness of the specimens was lower than 2 cm.

A contemporaneous archaeological study was carried out in the studied sites that allowed the dating of the combustion structures by different methods; archaeological constraints based on pottery and stratigraphic correlations, calibrated radiocarbon (^{14}C) and thermoluminescence (TL) techniques. TL dating was carried out directly on samples from the combustion structures. Half of the combustion structures were sampled for archaeomagnetic analysis and half for TL dating. The materials used for radiocarbon dating were charred material, charcoals, bone collagen and tooth found inside the huts or nearby the combustion structures. The dated materials belong in all cases to the stratigraphic layers of the hearths and kilns (archaeologist's personal communication).

The dating of the structures give ages ranging from 1200 BC up to 150 AD. TL dating was performed at the Centre for Nuclear Sciences and Technologies (C2TN) of the University of Lisbon and ^{14}C radiocarbon dating by Beta Analytic Inc. Calibration was conducted with INTCAL13 (Reimer et al., 2013). QCR12, CASTA1 and CASTA3 are the three oldest structures from the Late Bronze-First Iron Ages, with ages of 1210 ± 92 BC, 1100 ± 200 BC and 900 ± 200 BC, according to ^{14}C and TL dating. The youngest structure is the Roman kiln OPB. The remaining sites are from the Late Iron Age. A summary is provided in table 1.

In summary, the results from a total of 379 specimens coming from 151 independently oriented samples are presented in this study. Samples come from 33 archaeological combustion structures; 12 hearths and kilns from PCR (Povoado de Crestelos), 16 from QCR (Quinta de Crestelos), 1 from FM (Fonte do Milho), 1 from OPB (Olival Poço da Barca) and 3 from CAST (Castelinho).

The archaeomagnetic study was carried out at the Palaeomagnetism Laboratory of the Complutense University of Madrid. Minispin (Molspin) and JR5 (Agico) magnetometers were used to measure the natural remanent magnetization (NRM). Low field magnetic susceptibility (κ) of each specimen was measured using a KLY3 susceptibility meter (Agico). Stepwise thermal (TH) demagnetization of NRM was carried out using MMTD-80 and MMTD-24 (Magnetic Measurements) thermal demagnetizers. Stepwise alternating field (AF) demagnetization was conducted using a GSD-5 tumbling demagnetizer (Schonsted Instruments). A coercivity-spectrometer (Kazan University) was used to measure hysteresis loops, isothermal remanent magnetization (IRM) and backfield IRM, with a maximum applied field of 500 mT. Thermomagnetic curves were measured using a KLY3 kappabridge apparatus with a CS3 temperature control unit (Agico).

Pilot specimens from each structure were TH and AF demagnetized in 10 to 14 steps up to 600^{o}C or 100 mT respectively and κ of each specimen was monitored after each heating step. In addition, the thermal remanent magnetization anisotropy (ATRM) tensor was calculated for each specimen that was thermally demagnetized. The ATRM experiment was conducted when 60-70% of the natural remanent magnetization (NRM) was removed (typically around 400-450^{o}C, depending on the specimen). The ATRM tensor was calculated from the acquisition of a TRM in six different directions (specimen +X,-X, +Y,-Y, +Z,-Z), applying a laboratory field of 46 μT. Specimens from hearths and flat kilns were strongly anisotropic, with anisotropy corrections producing directional variations of the ChRM inclinations of up to 10°. Therefore, thermal treatment was preferred for the rest of the study and the anisotropy correction was systematically evaluated and applied to correctly estimate the archaeomagnetic directions.

3. Palaeomagnetic and rock magnetic results.

NRM intensities of the studied specimens range between 3 10^{-2} A/m and 3 A/m and the susceptibilities between 5 10^{-4} SI and 8 10^{-2} SI.

Figure 2 shows representative demagnetization diagrams from each of the studied sites, together with the normalized magnetization decays. The behaviour during TH and AF

demagnetizations was simple for the majority of specimens. Most of them exhibited a single stable magnetic component which was considered as the ChRM. This component was isolated between 100°C and (500–600)°C or 5 mT and (70-100) mT and comprised more than 90% of the initial NRM. The only exception was found in specimens from OPB, where 20% of the initial NRM remained after the 100 mT peak AF. This higher coercivity magnetization has the same direction as the lower coercivity magnetization (figure 2e). Exceptionally, some specimens showed overlapped components and were therefore rejected for the study.

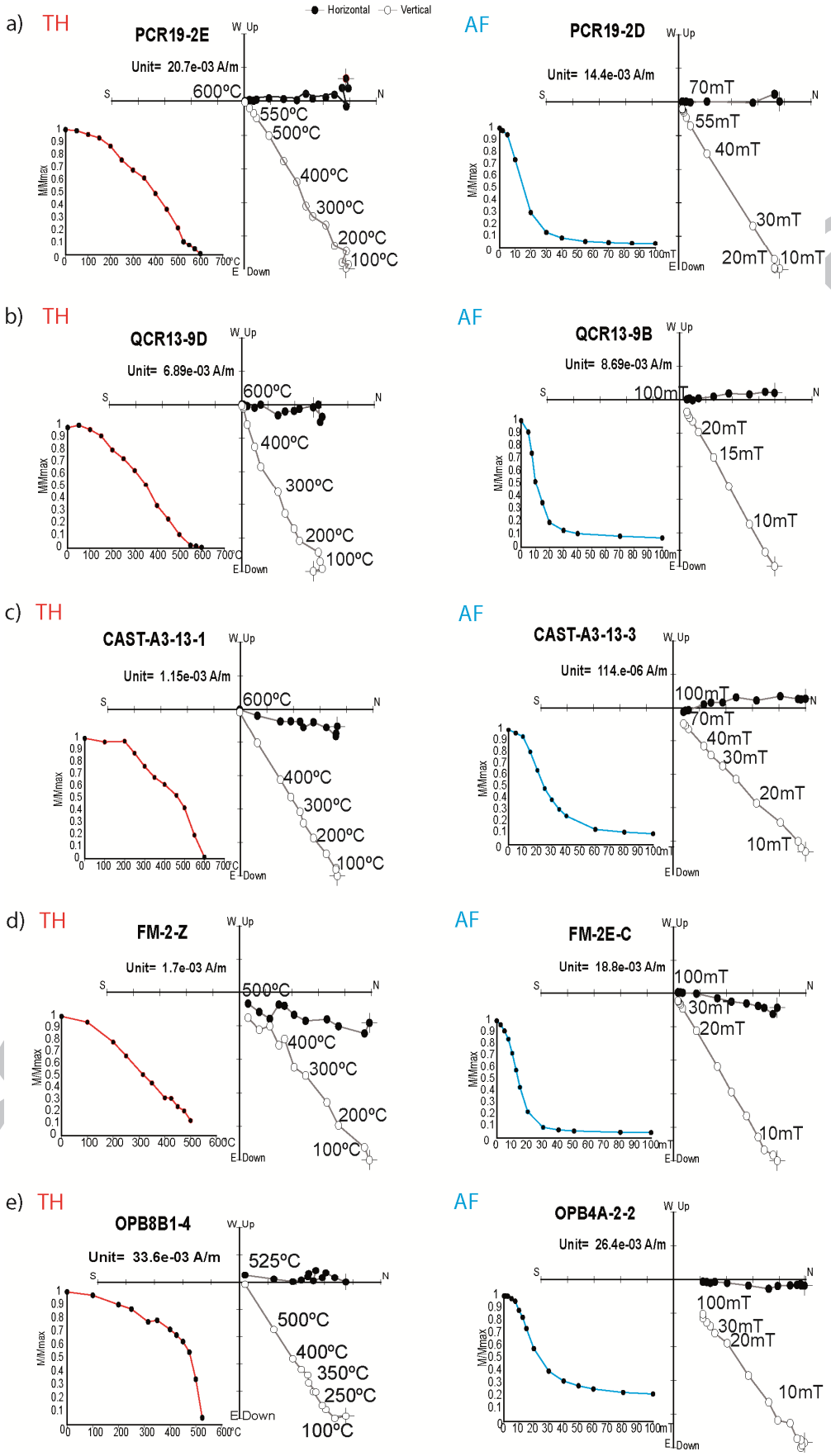

Figure 2: Orthogonal vector diagrams for NRM thermal (TH), alternating field (AF) demagnetization and normalized magnetization decays during demagnetization of representative specimens from the archaeological sites investigated: a) PCR, b) QCR, c) CAST, d) FM, e) OPB.

Hysteresis, IRM acquisition and back-field IRM curves were determined on representative specimens from all of the studied sites (figure 3). Saturation magnetisation (M_s), saturation remanent magnetisation (M_{rs}) and coercivity (H_c) were calculated from the hysteresis curves, while the coercivity of remanence (H_{cr}) was calculated from the backfield IRM curves.

Backfield IRM curves generally approached saturation in fields around -0.3 T, in agreement with the hysteresis curves. Contributions of higher coercivity minerals could be observed in some cases, being more clearly noticed in OPB specimens (e.g. figure 3e). H_{cr} varied between 6.5 mT and 47.1 mT, with OPB specimens having higher values than those from the other sites.

When plotted on a Day plot (Day et al., 1977, modified by Dunlop, 2002a), most data fell within the lower part of the pseudo-single-domain region (figure 3f), closely following the trends for single and multidomain mixture of magnetite (Dunlop, 2002a). The OPB data are slightly shifted compared to the rest of the data but followed a similar trend. This can be explained by the additional presence of high coercivity minerals. OPB is the only site with high M_s and IRM values that clearly show a high coercivity contribution to the IRM. The high coercivity fraction acts to increase H_{cr} and the H_{cr}/H_c ratio, shifting the points to the right of the Day plot compared to the other data.

Thermomagnetic curves from representative samples were predominantly non-reversible with maximum Curie temperatures between 515°C and 570°C (figure 3). The non-reversibility of the thermomagnetic curves is manifested by either a decrease in susceptibility after heating to 700°C (e.g. figure 3a), or an increase in it (e.g. figure 3d). A decrease in susceptibility is most likely due to oxidation, which typically occurs when clays are heated in air (Murad & Wagner, 1998). Increases in susceptibility could be explained by thermal decomposition of clay minerals and the formation of new magnetic phases. This might indicate that these specimens come from structures that have been previously heated to temperatures below 700°C. The univectorial nature of their NRM, however, strongly suggests that they were heated to at least 500-600°C.

The Curie temperatures are in close agreement with the maximum NRM unblocking temperatures. Together with the hysteresis and IRM results, this suggests that the NRM is dominated by low-Ti titanomagnetite or titanomaghemite and/or nearly pure magnetite. This is commonly observed in potteries and archaeological baked clays (Dunlop, 2002b).

An exception is seen for specimens from OPB, which show a clear influence of a high coercivity fraction. There is no evidence for the presence of hematite in the thermal demagnetization of NRM curves, nor in the thermomagnetic curves. There is some

suggestion of a change in slope of the NRM demagnetization curve around 250-300°C (e.g. figure 2e), which could indicate the presence of the HCLST phase identified by McIntosh et al. (2007) and would be consistent with the relatively large contribution to M_{rs} of the high coercivity fraction. However, the NRM demagnetization around 250°C is not very pronounced and this tentative interpretation would need to be confirmed with additional magnetic tests.

In summary, rock magnetic experiments and NRM demagnetization experiments suggest a magnetic mineralogy dominated by a mixture of single-domain and multidomain grains of low-Ti titanomagnetite or titanomaghemite and/or nearly pure magnetite as the main carriers of the NRM.

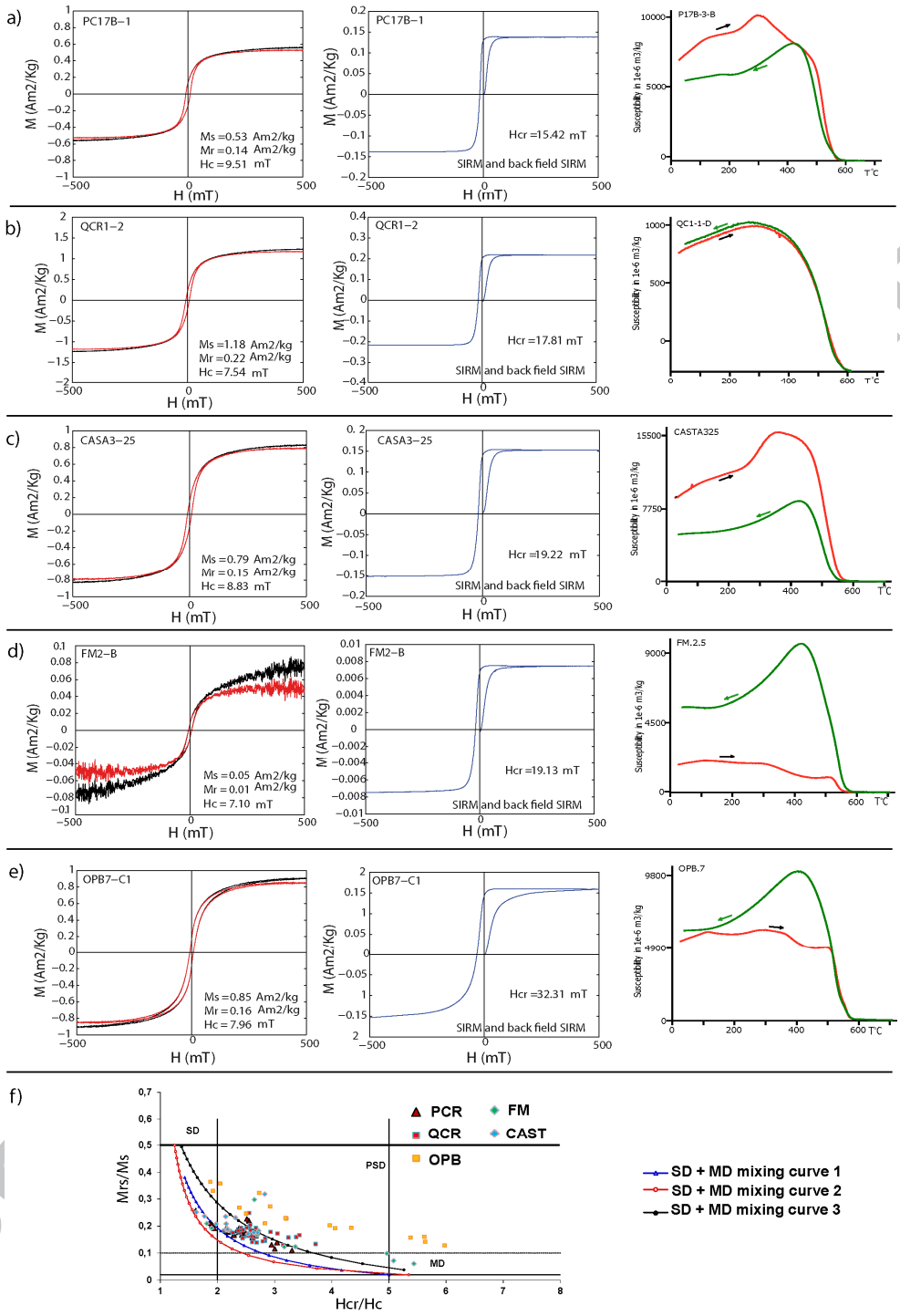

Figure 3: Left: Hysteresis curve (black and red curves/without and with paramagnetic contribution correction). Middle: IRM acquisition and backfield curve. Right: thermomagnetic curve, with heating/cooling shown in red/green. All data are normalized by mass. Data shown for a) PCR, b) QCR, c) CAST, d) FM and e) OPB sites. f) Day plot of hysteresis ratios with theoretical curves for mixtures of single domain (SD) and multidomain (MD) grains of magnetite (Day et al., 1977, modified by Dunlop, 2002a).

Archaeomagnetic directions were calculated from thermally demagnetized specimens with stable endpoints (with at least six linear steps) using principal component analysis (Kirschvink, 1980) and structure-mean directions were calculated using Fisherian statistics (Fisher, 1953). The small dimensions of most of the studied structures just allowed to collect a few number of independently oriented samples per site (table 1). Therefore, mean direction for each structure has been calculated based on the specimens and not on the samples mean value. All but two structures showed well-grouped directions with low semi-angles of confidence, α_{95}, and high precision parameters, k (with an average α_{95} value of 3.5 and 238 for k). Sites PC20A and PC26 exhibited the largest within-site dispersion of directions, with k values of 23 and 74 and α_{95} values of 9.8° and 7.0° respectively. Both were poorly preserved kilns and the dispersion is probably a result of undetected post-cooling movements of the fragmented baked layer. α_{95} values approaching 10° are very high for an archaeomagnetic study and as a consequence the PC20A and PC26 directions have not been not considered for further analyses.

Table 1 summarizes the location, archaeomagnetic directional results and the ages of all of the studied structures. Seven structures have calibrated radiocarbon (^{14}C) dating, seven thermoluminescence (TL) dating and the remaining ones have been archaeologically dated.

The ATRM was very high in most of the small kilns and hearths investigated. Table 1 also gives the average values of the anisotropy factor Pj (Jelinek, 1981). Pj values ranged from 1.159 at QCR9 up to 1.718 at QCR12, and in most structures they were higher than 1.300. In such highly anisotropic samples, the direction of the Earth's magnetic field can be deflected towards the easy axis of the specimens. Therefore the effect of anisotropy correction on the ChRM directions has been investigated and the ATRM correction has been applied for all specimens. In table 1, the mean directions before and after ATRM correction are shown.

The effect is illustrated in Figure 4, which shows ATRM ellipsoids from two specimens from the QCR5 structure, along with structure-mean ChRM directions before and after applying the anisotropy correction. The ATRM ellipsoids of the high anisotropic structures were oblate shaped with the minimum axes along the vertical. This shaped could explain that these structures registered lower inclinations values when the last thermorremanence process took place. It clearly shows that the two mean directions are statistically different, with no overlapping of the α_{95} semi-angles of confidence.

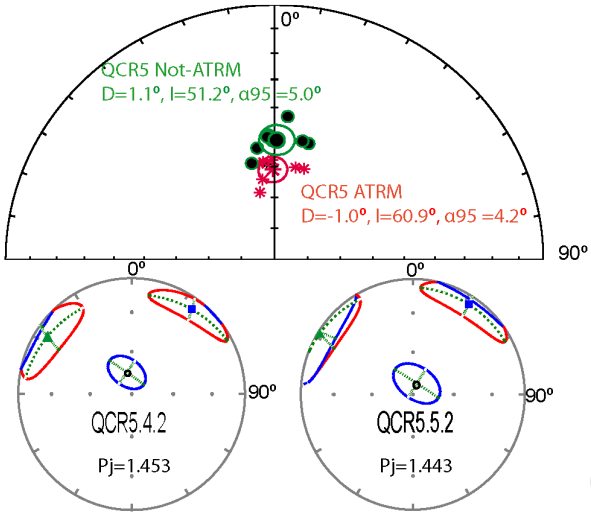

Figure 4: Equal area projection of mean directions of QCR5, before (green circles) and after (red stars) anisotropy correction was carried out, together with the α_{95} semi-angles of confidence and two examples of the ATRM ellipsoids of specimens QCR5.4.2 and QCR5.5.2.

The effect of anisotropy correction on the directions at the structure level is shown in figure 5, where inclinations and declinations are plotted before and after anisotropy correction. No systematic effects on declination values were observed when the anisotropy correction was carried out, with a mean average of the declination variation of -1° and a standard deviation of 3°. Systematic increases of the inclination values of between 2° and 13° were observed after anisotropy correction. The mean inclination shallowing of all the structures was 6°, with a standard deviation of 3°. Furthermore, the anisotropy correction slightly improved the α_{95} values (reducing them by 0.4° on average, with a standard deviation of 0.8°).

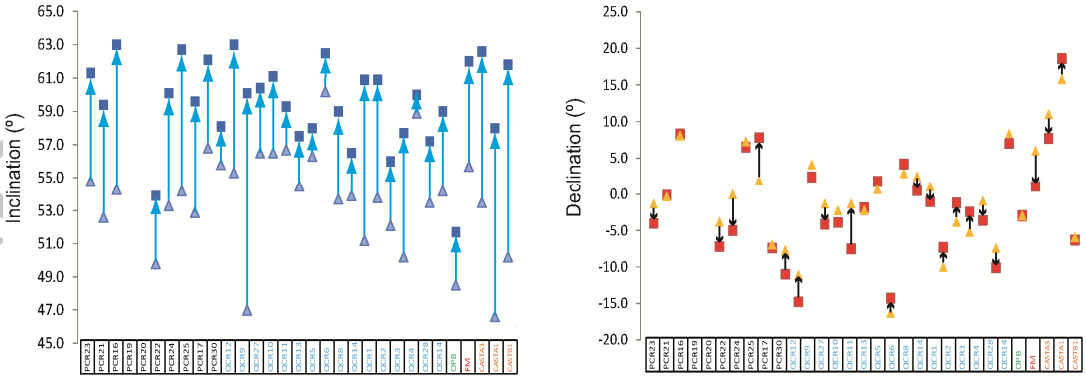

Figure 5: Inclination and declination values before (triangles) and after (squares) applying the anisotropy correction (structures in chronological order at site level).

TRM anisotropy corrections are determined in high quality palaeointensity studies (Chauvin et al., 2000, Gomez-Paccard et al., 2012, etc.). The effects that these corrections

apply in palaeiontensity values could be very strong, mainly in the case of ceramics, bricks and tiles. Regarding to the effects that ATRM corrections apply to palaeodirections, Tema (2009) observed systematic inclination shallowing on the directions of well dated ancient bricks. High anisotropy effects were also found by Hus et al., 2002; 2003 in bricks and tiles. On the contrary, low values of anisotropy on small hearths are described by Kovacheva et al., (2009) and Hervé et al., (2013). It is necessary to perform more systematic determinations of ATRM tensors in palaeodirectional studies to better understand this effect.

The results obtained from this study reveal that the TRM anisotropy effect could to be very important in the base of thin, flattened kilns and hearths. They highlight the fact that anisotropy must be systematically investigated and properly corrected for in these types of archaeological materials. We suggest that the origin of this ATRM could be the pressure applied to the sediments (that were used as the basin of the combustion structures) during the construction processes.

4. Discussion.

4.1 The Iberian and SW European archaeomagnetic database 1200 BC-200 AD.

Figure 6a shows the 31 accepted directional data from this study plotted versus time (in situ coordinates, without any relocation). There are three data from 1200 BC to 900 BC and 28 data from 300 BC to 200 AD, with a 600 year gap between them. North-easterly declinations are observed for the oldest structures, with declinations increasing towards 900 BC. The younger group has declination close to zero with dominant north-westerly values. Inclination values are fairly constant across the whole of the time period represented by the structures, remaining between 65^{o} and 55^{o}. The lowest inclination is observed for the youngest (Roman) site. Figure 6b and table 1S (supplementary material) summarize all available data for Iberia for the period 1200 BC up to 200 AD, relocated to Madrid coordinates using the virtual geomagnetic pole method (Noël and Batt, 1990). A total of 63 data from Iberia are summarized for this time span, the 31 data from this study together with 31 previously published data. It is important to note that the majority of the 31 previous Iberian data are from the Roman period: 30 data are from 100 BC up to 200 AD, one from central Iberia from 180 BC (Osete et al., 2016) and one provided by Catanzariti et al. (2008) from 850 BC. The dataset summarized in table 1S excludes three previous studies that have not been considered for this study. Firstly, an archaeomagnetic study performed by Casas et al. (2014) focusing on archaeomagnetic dating has been omitted because no independent dating information was provided. Secondly, one of the results of Carrancho et al. (2013) has been excluded, since they describe results from a site with a 900 year radiocarbon dating error interval. Finally, one of the results of Ruiz-Martinez et al. (2008) has been excluded because the authors highlight that has been affected by, but not corrected for, inclination shallowing. No other quality or selection criteria have been applied in this section. The resulting Iberian catalogue is shown in figure 6b. There is very good agreement between the data, both for the younger, post-400 BC directions and for the older, pre-800 BC directions. However, there is still a gap in the data between 850 BC and 300 BC.

In order to fill this gap it is necessary to include data from neighbouring regions and for this purpose data falling within a 900 km radius of Madrid have also been considered. This new dataset is shown in figure 6c, with all directions relocated to Madrid coordinates. It includes 60 data from southern France and 2 from northern Morocco. No quality or selection criteria were applied to this data. Both French and Moroccan data show a good agreement with the Iberian data (figure 6c). While it is noticeable that most of the neighbouring data are also concentrated in the 300 BC to 200 AD time interval, there are 15 directions that are older and that help to fill in the gap between 850 BC and 300 BC.

The updated southwestern European archaeomagnetic catalogue, summarized in figure 6c and table 1S (Supplementary material), shows remarkable consistency. This permits a broad description of the evolution of the geomagnetic field for a nearly 1500-year period between 1300 BC and 200 AD. A large eastward–westward declination swing is seen that reaches a maximum declination of around 30^{o} at 800 BC, followed by a period of fairly uniform declination between 400 BC and 200 AD. Inclination reaches a maximum value of nearly 70^{o} at about 650 BC, and then gradually decreases to around 45^{o} by 200 AD.

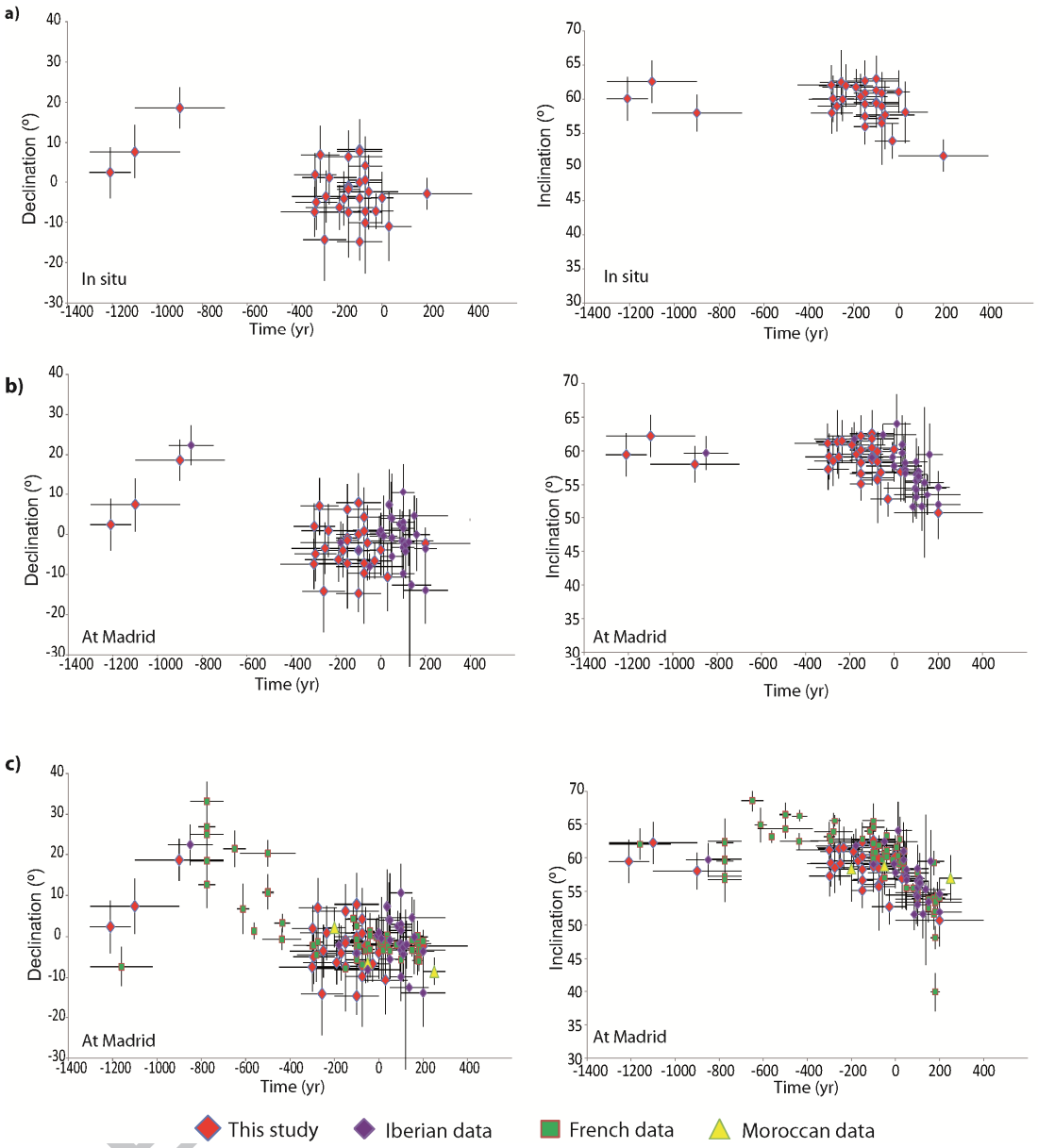

Figure 6: Declination and inclination versus time. a) New data from this study (in situ coordinates, without any relocation); b) New data plus data from other Iberian sites (relocated at Madrid coordinates); c) New data plus data from Iberian, French and Moroccan sites located inside a 900 km radius centred on Madrid (at Madrid coordinates).

4.2 The PSV for the Iberian Peninsula from Late Bronze Age to Roman Times.

A new PSV curve for the Iberian Peninsula (figure 8a-b) has been computed using the bootstrap method (Korte and Constable, 2008; Thébault and Gallet, 2010). In order to

homogenise the database, the curve was constructed including data from the previously presented SW European catalogue that passed the following quality criteria: 1) the number of specimens per structure was greater than or equal to 4; 2) the α_{95} value was lower than or equal to 5^{o}; 3) the age uncertainties were lower than ±250 years. Following these quality criteria seven Spanish data, one French data and four Moroccan data were rejected, leaving a total of 120 good quality data (55 Iberian, 4 northern Moroccan and 61 southern French data, see figure 7) that were relocated to Madrid coordinates using the virtual geomagnetic pole method (Noël and Batt, 1990).

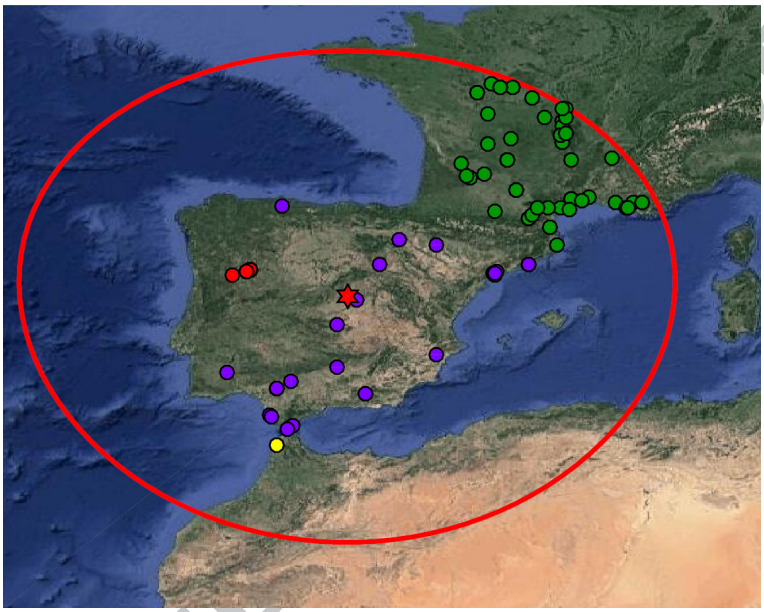

Figure 7: Spatial distribution of the selected dataset located inside a 900 km radius centred at Madrid (red star): This study (in red), Iberian (in purple), Moroccan (in yellow) and French (in green) data.

A set of 5000 individual PSV curves for declination and inclination were generated following the bootstrap method. The original archaeomagnetic database and penalised cubic B-splines in time were used. For each bootstrap curve, synthetic data were obtained from two different probability distributions: 1) a random Gaussian probability function centred on the original directional value and with a standard deviation equal to the directional uncertainty (α_{65}) and 2) a random homogeneous distribution with amplitude given by the time error at 1σ, in time. The final directional PSV curve was calculated as the average of these 5000 individual curves along with their standard deviation (at the 95% level of confidence). The cubic B-splines base was determined using knot points every 50 years between 1200 BC and 200 AD and regularized by an additional penalty function, which controls the trade-off between the input data and the roughness of the estimated directional curve. This function was chosen as the second derivative of the estimated function (the PSV curve) multiplied by a damping parameter, which controls the regularization. If this parameter is too high, the smoothing of the curve will be overestimated. On the contrary, if the damping parameter is too low, the regularization

will have no effect and the variability of the curve will be unrealistic. The optimum parameter will be located in the knee point in the curve of the root mean square error between the original and estimated data from the PSV curve as a function of different damping parameters (figure 1S in the supplementary material).

The obtained Iberian directional PSV curve is shown in figure 8a-b. Figure 8a shows the value of the declination versus time, which moves from values close to zero in 1200 BC, towards easterly values from 1200 BC to 800 BC and reaching a maximum of 23^{o} E. This is followed by a westerly trend up to 2^{o} W at 300 BC. From 300 BC to 200 AD, small fluctuations in declination are observed. In figure 8b inclination versus time shows a slight decrease between 1200 BC and 800 BC, then a more rapid increase to maximum values around 65^{o} at 600 BC, before decreasing again to around 50^{o} by 200 AD.

The new Iberian PSV curve has been compared with the recently proposed PSV curve for Western Europe (Hervé et al., 2013), with the European regional model SCHA.DIF.3k (Pavón-Carrasco et al., 2009) and with global models (Pavón-Carrasco et al., 2014; Korte et al., 2009; Korte and Constable, 2011). This comparison is illustrated in figure 8c-f.

The Western European PSV curve (Hervé et al., 2013) was built using a bivariate extension of Fisher statistics (Le Goff, 1990; Le Goff et al., 1992). It was constructed from 204 data with ages ranging between 1500 BC and 200 AD and located within 1000 km of Paris. Data were selected from the Geomagia50v2 database (Donadini et al., 2009) and come from the United Kingdom, Germany, Switzerland, Austria, Italy and Spain. Quality criteria based on the number of specimens per structure (higher than 2), the α_{95} value (lower than 5^{o}) and the age uncertainties (lower than ± 250 years) were applied. The Iberian curve is highly consistent with the Western European curve of Hervé et al. (2013) relocated to Madrid coordinates. But it is important to note that 53% of the data used to build the new Iberian PSVC were also included in the Western Europe PSV curve. The larger amount of data (and its better temporal distribution) used to generate the Western European curve leads to a lower uncertainty interval than the Iberian curve. This is especially important for times before 800 BC. However, both curves are statistically indistinguishable.

The European model SCHA.DIF.3k (Pavón-Carrasco et al., 2009), which describes the evolution of the Earth's magnetic field from 1000 BC up to 1900 AD at a continental scale, was developed by inversion of European archaeomagnetic data using spherical cap harmonic analysis (SCHA) in space and sliding windows in time. It was based on archaeomagnetic data published up to 2008. Therefore the new French data were not included, but it included data from the whole European region. The selection criteria used was to reject all directional data whose α_{95} was three times bigger than the mean α_{95} and all intensity data whose σ_F was three times the mean σ_F. After applying this filter, 1437 declination, 1979 inclination and 913 intensity data remained and were used to construct the model. There is a good fit between the synthetic PSV curve provided by the SCHA.DIF.3k model in Madrid coordinates and the new Iberian PSV curve proposed in this study (figure 8c-d). Although the SCHA.DIF.3k model seems to slightly overestimate the inclination maximum around 600 BC, both curves are statistically indistinguishable.
Finally, figure 8e-f compares the Iberian PSVC with the synthetic curves provided by global models SHA.DIF.14k (Pavón-Carrasco et al., 2014), ARCH3k.1 (Korte et al., 2009)

and CALS3k.4b (Korte and Constable, 2011) computed at Madrid coordinates. The global models SHA.DIF.14K and ARCH3K.1 were generated by regularized least-squares inversion using archaeomagnetic and volcanic data, spherical harmonics analysis (SHA) in space until degree 10 and cubic B-splines in time. In contrast, the CALS3k.4b model also includes sedimentary data.

As expected, the PSVC at Madrid derived from the global SHA.DIF.14K and ARCH3K.1 models are highly consistent since both are based on similar input data and modelling methods. The CALS3k.4b model produces a markedly different secular variation curve, reflecting the smoothness produced by the inclusion of the sedimentary data.

Global models tend to show a higher temporal variability than observed in the Iberian PSV curve (figure 8e-f). There is a general agreement in the declination curves, with a maximum easterly value reached around 800 BC. The inclination curves, however, do not fit so well for times prior to 400 BC. Global models present a minimum value around 600 BC, whilst the Iberian curve presents a broad maximum that is also observed in the Western European PSV curve and in the regional European model. This means that the inclination minimum around 600 BC is mainly controlled by data coming from outside the western European region. In fact, this minimum could be related to data coming from the region around Sofia, Bulgaria (see figure 2S in the supplementary material). It would be important to focus future archaeomagnetic studies in Western Europe in this time interval in order to discriminate if the double peak in inclination showed by the global models at 800 BC and 450 BC is a global feature of the geomagnetic field or a local characteristic of the eastern European region. In addition, attention should be paid to the potential role of inclination shallowing in producing minimum values in inclination PSV curves. As the present study has shown, this could have a significant impact on the inclinations recovered from sites and structures of similar type.

In summary, and despite the scarcity of data for periods preceding 300 BC, the new PSV curve for Iberia for the first millennium BC proposed in this study is in general accordance with the Western European PSV curve and the regional European model. All the descriptions of the evolution of the Earth's magnetic field in SW Europe that are based on local archaeomagnetic data or regional and global modelling are consistent from 400 BC up to 200 AD. Discrepancies in inclination values are observed prior to these times. New data are still necessary to adequately describe the evolution of the field during the first half of the first millennium BC.

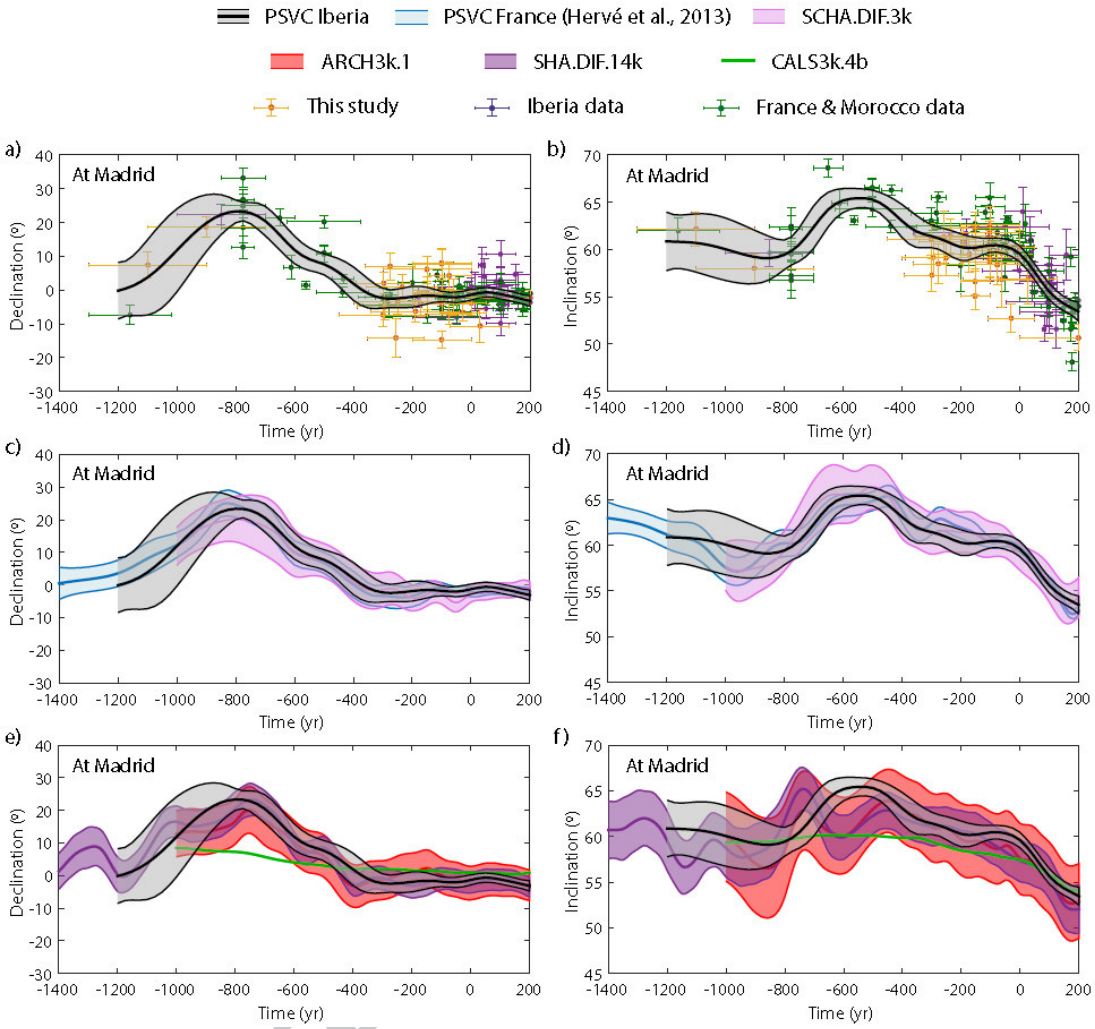

Figure 8: a-b) PSVC (Declination-Inclination) based on data inside a 900 km radius from Madrid*; c-d) PSVC (Declination-Inclination) of this study, Hervé et al. (2013) and SCHA.DIF.3k; e) and f) PSVC of this study, ARCH3k.1, SHA.DIF.14k, CALS3k.4b. The error bands are given at 95% of confidence level.*

5. Conclusions.

High quality archaeomagnetic directions have been obtained from 31 of the 33 combustion structures investigated at four archaeological sites from northern Portugal. The new data greatly improve the temporal distribution of archaeomagnetic data of the Iberian Peninsula. The effect of TRM anisotropy on directions has been evaluated and shown to be important, emphasizing the requirement of evaluating this effect on archaeomagnetic studies carried out on small kilns and thin hearths. This study has allowed the construction of a new directional PSV curve for Iberia for the first millennium BC up to 200 AD, computed using the bootstrap method and including data filtered by

quality criteria and coming from sites located inside a 900 km radius centred on Madrid. The new PSV curve for Iberia is consistent with the Western European PSV curve and with the regional European model, SCHA.DIF.3k. It is well defined for the period between 400 BC and 200 AD, when the local and regional curves from Western Europe agree with the global descriptions of the geomagnetic field. Finally, it is worth reiterating the need to increase the number of directional archaeomagnetic data for Iberia for the period between 1200 BC and 300 BC, for which data is still sparse.

Acknowledgements

The authors are grateful to the Spanish Research Project CGL2014-54112-R which has supported the field and laboratory costs, as well as the post-doctoral contract of APO. We would also thanks all the people involved in the field and laboratory work. We also would like to thank E. Tema and anonymous reviewer for improving the paper.

References.

AHBS Empreitada Geral de Construsao do Aproveitamento Hidroeléctrico do Baixo Sabor. 2014. Plano de Salvaguarda do património estudo da idade do Ferro no Baixo Sabor. 613pp.

Day, R., Fuller, M., Schmidt. V. A. 1977. Hysteresis properties of titanomagnetites: Grain size and composition dependence. Phys. Earth Planet. Inter. 13, 260–267.

Donadini, F., Korte M., Constable C.G. 2009. Geomagnetic field for 0-3 ka: 1. New data sets for global modelling. Geochemistry, Geophysics, Geosystems, 10.

Dunlop, D.J. 2002a. Theory and application of the Day plot (Mrs/Ms versus Hcr/Hc). 1. Theoretical curves and tests using titanomagnetite data, J. Geophys. Res., 107(B3), doi: 10.1029/2001JB000486. EPM 4.1–4.22.

Dunlop, J. 2002b. Theory and application of the Day plot (Mrs/Ms versus Hcr/Hc). 2. Application to data for rocks, sediments, and soils David Theoretical curves and tests using titanomagnetite data. J. Geophys. Res. 107 (B3), 2057.

Cambridge Publication. In press. Archaeology in the River Duero valley (Spain and Portugal): From Paleolithic to Medieval Age. New perspectives and advance in the investigation of the past.

Catanzariti, G., McIntosh, G., Monge Soares, A. M., Díaz-Martínez, E., Kresten, P., Osete, M. L. 2008. Archaeomagnetic dating of a vitrified wall at the Late Bronze Age settlement of Misericordia (Serpa, Portugal). Journal of Archaeological Science, 35, 1399-1407.

Catanzariti, G., Gómez-Paccard, M., McIntosh, G., Pavón-Carrasco, F.J., Chauvin, A., Osete, M.L. 2012. New archaeomagnetic data recovered from the study of Roman and Visigothic remains from central Spain (3rd-7th centuries). Geophys. J. Int., 188, 979-993.

Carrancho A., Villalain J.J., Pavon-Carrasco F.J., Osete M., Straus L., Verges J., Carretero J., Angelucci D., Gonzalez-Morales M., Arsuaga J., Bermudez-Castro J., Carbonell E. 2013. First directional European palaeosecular variation curve for the Neolithic based on archaeomagnetic data. Earth Planet. Sci. Lett., 380, 124-137, doi: 10.1016/j.epsl.2013.08.031.

Casas Ll., Prevosti M., Fouzai B., Alvarez A. 2014. Archaeomagnetic study and dating at five sites from Catalonia (NE Spain). J. Arch. Sci., 41, 856-867, doi: 10.1016/j.jas.2013.10.020.

Chauvin, A., Garcia, Y., Lanos, Ph., Laubenheimer, F. 2000. Paleointensity of the geomagnetic field recovered on archaeomagnetic sites from France. c. Physics of the Earth and Planetary Interiors. 120, 111–136.

C2TN (Centro de Ciencias y tecnologías Nucleares). 2014. Relatroio dinal da intervensao científica: Cronoestratigrafia em problemáticas arqueológicas identificadas na área de afectasao da construsao da barragem do Sabor.

Fisher, R.A. 1953. Dispersion on a sphere, Proc. Roy. Soc. Lond. Ser. A. 217,295–305.

Gallet, Y., Hulot, G., Chulliat, A., Genevey, A. 2009. Geomagnetic field hemispherica symmetry and archaeomagnetic jerks. Earth Planet. Sci. Lett. 284,179–186.

Gómez-Paccard, M., Catanzariti, G., Ruiz-Martinez, V. C. McIntosh, G., Núñez, J. I., Osete, M. L., Chauvin, A., Lanos, P., Tarling, D. H., Bernal-Casasola, D., Jacques. T. 2006a. A catalogue of Spanish archaeomagnetic data. Geophysics Journal International, 166, 1125-1143.

Gómez-Paccard, M., Chauvin, A., Lanos, P., McIntosh, G., Osete, M. L., Catanzariti, G., Ruiz-Martinez, V. C., Núñez, J. I. 2006b. First archaeomagnetic secular variation curve for the Iberian Peninsula: comparison with other data from Western Europe and with global geomagnetic field models. Geochemistry, Geophysics, Geosystems. 7, Q12001, http://dx.doi.org/10.1029/2006GC001476.

Gómez-Paccard, M., Chauvin, A., Lanos, P., Thiriot, J. 2008. New archeointensity data from Spain and the geomagnetic dipole moment in western Europe over the past 2000 years. Journal of Geophysical Research, 113, B09103, doi :10.1029/2008JB005582.

Gomez-Paccard, M., McIntosh, G., Chauvin, A., Beamud, E., Pavón-Carrasco, F.J., Thiriot, J., **2012**. Archaeomagnetic and rock magnetic study of six kilns from North Africa (Tunisia and Morocco). **Geophysical Journal International**, 189, 169-186

Gómez-Paccard, M., Gregg, M., Beamud, E., Larrasoaña, J. C. 2013. New archaeomagnetic data recovered from the study of three Roman kilns from north-east Spain: A contribution to the Iberian Palaeosecular variation curve. Archaeometry. 55 - 1, pp. 159 - 177.

Hervé, G., Chauvin A., Lanos, P. 2013. Geomagnetic field variations in Western Europe from 1500BC to 200AD. Part I: Directional secular variation curve. Physics of the Earth and planetary Interiors, 218, 1-13.

Hus, J., Ech-Chakrouni, S., Jordanova, D., 2002. Origin of magnetic fabric in bricks: its implications in archaeomagnetism. Phys. Chem. Earth, 27, 1319-1331.

Hus, J., Ech-Chakrouni, S., Jordanova, D., Geeraerts, R., 2003. Archaeomagnetic investigation of twomediaeval brick constructions in North Belgium and the magnetic anisotropy of bricks. Geoarchaeology, 18, 225–253.

Jelinek, V. 1981. Characterization of the magnetic fabrics of rocks. Tectonophysics 79:T63–T67.

Kirschvink, J.J. 1980. The least-squares line and plane and the analysis of paleomagnetic data. Geophys. J. R. Astr. Soc., 62, 699–718.

Korte, M., Constable, C. 2008. Spatial and temporal resolution of millennial scale geomagnetic field models. Adv. Space Res. 41, 57–69. http://dx.doi.org/10.1016/j.asr.2007.03.094.

Korte, M., Donadini, F., Constable, C. G. 2009. Geomagnetic field for 0-3 ka: 2. A new series of time-varying global models. Geochem. Geophys. Geosyst., 10, Q06008 , doi:10.1029/2008GC002297.

Korte, M., and Constable, C.G. 2011. Improving geomagnetic field reconstructions for 0-3 ka. Phys. Earth Planet. Interiors. 188, 247-259.

Kovacheva, M., Chauvin, A., Jordanova, N., Lanos, Ph., Karloukovski, V., 2009. Remanence anisotropy effect on the palaeointensity results obtained from various archaeological materials, excluding pottery. Earth Planets Space 61, 711–732.

Lanza R., Meloni A., Tema E. 2005. Historical measurements of the Earth's magnetic fieldcompared with remanence directions from lava flows in Italy over the last four centuries. Physics of Earth and Planetary Interiors, 148, 97-107.Le Goff, M. 1990. Lissage et limites d'incertitude des courbes de migration polaire: pondération des données et extension bivariate de la statistique de Fisher. C.R. Acad. Sci. Paris, 311 (Serie II) pp. 1191–1198.

Le Goff, M., Henry, B., Daly, L. 1992. Practical method for drawing a VGP path. Phys. Earth Planet. Int. 70, 201–204.

McIntosh, G., Kovacheva, M., Catanzariti, G., Osete, M.L. & Casas, L. 2007. Widespread occurrence of a novel high coercivity, thermally stable, low unblocking temperature magnetic phase in heated archeological material, Geophys. Res. Lett., 34, L21302, doi:10.1029/2007GL031168.

Murad, E. & Wagner, U. 1998. Clays and clay minerals: The firing process, Hyperfine Interactions, 117, 337-356.Muscheler, R., Joos, F., Beer, J., Müller, S.A., Vonmoos, M., Snowball, I. 2007. Solar activity during the last 1000 yr inferred from radionuclide records. Quat. Sci. Rev.,26, 82–97.

Noël, M. and Batt, C.M. 1990. A method for correcting geographically separated remanence directions for the purpose of archaeomagnetic dating. Geophys. J. Int. 102,753–756.

Osete, M.L., Chauvin, A., Catanzariti, G., Jimeno, A., Campuzano, S.A., Benito-Batanero, J.P., Tabernero-Galán, C., Roperch, P. 2016. New archaeomagnetic data recovered from the study of celtiberic remains from central Spain (Numantia and Ciadueña, 3rd-1st BC). Implications on the fidelity of the Iberian palaeointensity database. Phys. Earth. Planet. Inter. (260), 74-86.

Pavón-Carrasco, F. J., Osete, M. L., Torta, J. M., Gaya-Piqué L. R. 2009. A regional archaeomagnetic model for Europe for the last 3000 years, SCHA.DIF.3K: Applications to archaeomagnetic dating. Geochemistry Geophysics Geosystems, 10 (3).

Pavón-Carrasco, F. J., Rodríguez-González, J., Osete, M.L., Torta, J. M. 2011. A Matlab tool for archaeomagnetic dating. Journal of Archaeological Science, 38, 408-419.

Pavón-Carrasco, F. J., Osete, M.L., Torta, J. M., De Santis, A. 2014.A geomagnetic field model for the Holocene based on archaeomagnetic and lava flow data. Earth and Planetary Science Letters, 388, 98–109.

Pavón-Carrasco F.J., Tema E., Osete M.L., Lanza R. 2016. Statistical Analysis of Palaeomagnetic Data from the Last Four Centuries: Evidence of Systematic Inclination Shallowing in Lava Flow Records. Pure and Applied Geophysics. Volume: 173, Issue: 3, Publisher: Birkhauser Verlag AG, Pages: 839-848.

Prevosti M., Casas Ll., Roig-Perez J.F., Fouzai B., Alvarez A., Pitarch A. 2013 Archaeological and archaeomagnetic dating at a site from the ager Tarraconensis (Tarragona, Spain): El Vila-sec Roman pottery. J. Arch. Sci., 40, 2686-2701, doi: 10.1016/j.jas.2013.01.027.

Reimer, P.J., Bard, E., Bayliss, A., Beck, J.W., Blackwell, P.G., Bronk Ramsey, C., Buck, C.E., Cheng, H., Edwards, R.L., Friedrich, M., Grootes, P.M., Guilderson, T.P., Haflidason, H., Hajdas, I., Hatté, C., Heaton, T.J., Hoffmann, D.L., Hogg, A.G., Hughen, K.A., Kaiser, K.F., Kromer, B., Manning, S.W., Niu, M., Reimer, R.W., Richards, D.A., Scott, E.M., Southon, J.R., Staff, R.A., Turney, C.S.M., Van der Plicht, J. 2013. IntCal13 and Marine13 radiocarbon age calibration curves 0–50,000 years cal BP. Radiocarbon *55(*4):1869–1887.

Roberts, A. P., Tauxe, L., Heslop, David. 2013. Magnetic paleointensity stratigraphy and high-resolution Quaternary geochronology: successes and future challenges. Quaternary Science Reviews 61 1-16.

Ruiz-Martínez, V. C., Pavón-Carrasco, F. J., Catanzariti, G. 2008. First archaeomagnetic data from northern Iberia. Physics and Chemistry of the Earth, 33, 566-577.

Tauxe, L. 1993. Sedimentary records of relative paleointensity of the geomagnetic field: theory and practice. Rev. Geophys., 31, 319–354.

Tema, E., 2009. Estimate of the magnetic anisotropy effect on the archaeomagnetic inclination of ancient bricks. Physics of Earth and Planetary Interiors, 176, 213-223.

Thébault, E., Gallet, Y. 2010. A bootstrap algorithm for deriving the archaeomagnetic field intensity variation curve in the Middle East over the past 4 millennia BC. Geophys. Res. Lett., 37, L22303, doi: 10.1029/2010GL044788.

Usoskin, I. G., Kromer, B., Ludlow, F., Beer, J., Friedrich, M., Kovaltsov, G. A., Solanki, S. K., Wacker, L. 2013. The AD775 cosmic event revisited: The Sun is to blame. Astron. Astrophys. 552, L3, doi:10.1051/0004-6361/201321080.

Highlights.

- Great improving of the archaeomagnetic dataset of the Iberian Peninsula for the first millennium BC.
- 31 new high quality palaeodirectional data from Portugal obtained from archaeological combustion structures.
- New paleosecular variation curve for Iberia for the first millennium BC up to 200 AD, computed using the bootstrap method.